Anyanwu *et al.*: Nigerian Journal of Materials Science and Engineering. Vol. 14 (1): 8-16 (2024)

Electrochemical Impact of Zinc-Magnesium Oxide-Cellulose Nano-particle Electrodeposited Composite Coatings on Low Carbon Steel in Sodium Chloride Media

[1*]Anyanwu B.U., [2]Owoeye S.O., [1]Olamide O.O., [1]Olaitan K.L., [1]Anibaba A.D., [3]Yussouff A.A. and [1]Okpako O.
[1.]Mechanical Engineering Department, Federal University of Agriculture, Abeokuta, Nigeria.
[2.]Mechatronics Engineering Department, Federal University of Agriculture, Abeokuta, Nigeria.
[3.]Industrial and Systems Engineering Department, Lagos State University, Lagos, Nigeria.
*Correspondence e-mail: anyanwubu@funaab.edu.ng

Abstract
Low-carbon steel (LCS) is applied in numerous engineering applications, such as construction, automobile manufacturing, and product and component manufacturing, due to its unique mechanical properties. They are readily available, hence are very cost-effective when considered in any application. However, they are usually affected by corrosion when exposed to chloride-induced media, due to the penetration of chloride ions. Biopolymer coatings electrodeposited on the surface of metals have been shown to restrict the penetration of chloride ions into the metallic substrate, thereby slowing down the corrosion rate. This study was aimed towards electrodepositing Zinc-magnesium oxide-cellulose nano-particle coatings (Zn-xMnO-xC_n) on LCS for improved corrosion resistance in sodium chloride media. The gravimetric technique was used to determine the corrosion rates of the deposited coatings (samples). The samples' morphology and composition were determined via optical microscopy and scanning electron microscopy, equipped with an energy-dispersive spectrometer. Corrosion data from the results showed that all the coatings recorded lower corrosion rate values than that of the LCS substrate, whose value was 5.0025 mm/y. Among the coatings, sample M10 (Zn-20gMgO-20gC_n) had the least corrosion rate value of 0.2582 mm/y, corresponding to a coating protection efficiency of 95% on the LCS. The highest corrosion rate value was recorded by M7 (Zn-20gMgO-5gC_n) with a value of 2.2236 mm/y corresponding to a protection efficiency of 56% on the LCS. The coating morphologies revealed uniformly distributed and fine grains on the LCS' surface. The study showed that the Zn-xMnO-xC_n coatings were able to form protective barriers on the substrate in the sodium chloride media.

Keywords: Chloride, ions, coatings, substrates, corrosion

1.0 INTRODUCTION:

Corrosion is the slow degradation or breakdown of materials, typically metals, resulting from chemical or electrochemical interactions with their surroundings. This process results in the conversion of the metal into a more stable compound, such as an oxide, hydroxide, or sulfide (Ibrahimi *et al*., 2021). Despite its extensive use in various engineering applications, low-carbon steel is highly susceptible to corrosion, particularly in chloride-rich environments such as seawater. This has led to substantial safety challenges and economic losses (Feng *et al*., 2021; Mi *et al*., 2023).

Chloride-induced corrosion of low-carbon steel in sodium chloride environments occurs because chloride ions negatively impact the protective oxide layer on the steel (El-Sherik, 2016). Chloride ions pierce the oxide layer and react with the metal when they come into contact with the steel surface. This process produces corrosion products like iron chloride (Fan *et al*., 2022).

The corrosion process is affected by several factors, including temperature, pH, and chloride ion concentration. Elevated temperatures speed up the corrosion rate, whereas low pH levels and high chloride concentrations intensify the corrosiveness of the environment. Furthermore, impurities and other corrosive substances can exacerbate the corrosion process (Cai *et al*., 2020; Obot *et al*., 2023; Zehra *et al*., 2022; Patra, 2019).

A number of studies have been carried out in an attempt to comprehend the mechanisms underlying the chloride-induced corrosion of low-carbon steel. Reports by Zhang (2015) suggest that the corrosion process begins with the formation of small pits on the steel surface, which subsequently spread and form larger corrosion sites. The presence of chloride ions speeds up the rate at which these pits propagate, causing the steel to corrode more quickly. The pH of sodium chloride media can also affect the rate of corrosion. Research by Patra (2019) reported that lower pH and highly acidic environmental conditions make the environment housing steel products and applications more aggressive, thereby resulting in higher corrosion rates. This is explained by the fact that there are more hydrogen ions available, which facilitate iron breakdown and the production of corrosion products (Smith and Craig, 2020).

Another important factor influencing low-carbon steel corrosion is the concentration of chloride ions in the media. An atmosphere with higher amounts of chloride is more likely to be corrosive because there is a greater chance of chloride penetrating the oxide layer and reacting with the metal (Song *et al*., 2017; Wasim *et al*., 2018). These challenges, therefore, continue to make corrosion and material experts consistently strive to devise innovative methods to enhance the structural integrity of low carbon steel across various applications, including domestic, industrial, automotive, marine, and agro-allied processing, whether in chloride, alkaline, or acidic environments (Anyanwu *et al*., 2021; Fayomi *et al*., 2021; Abbas and Shafiee, 2020).

Several corrosion preventive measures have been researched in recent times, but the development of effective corrosion-resistant composite coatings on metals by electro-deposition technique is a critical area of research aimed at enhancing the performance and lifespan of low-carbon steel structures. This is because the method is simple to use, has near near-zero carbon footprint and low energy consumption. The technique has been found not only to reduce the corrosion rates of metals in aggressive media, but also to improve their mechanical properties, depending on the coating materials (Anyanwu *et al*., 2023a; Odetola *et al*., 2016; Popoola and Fayomi, 2012).

Coating by electro-deposition is an electrochemical process applied in surface structure modification. It is a cost-effective surface modification method for the deposition of organic and synthetic coatings on metallic materials (Praveeen and Venkatesh, 2011). In a typical electro-deposition process, monolayer or multilayer coatings are formed because of the electrochemical reactions occurring at the electrode/electrolyte interface and ion deposition from the electroplating bath.

Coatings are applied to materials (substrates) through electro-deposition to enhance properties such as corrosion resistance, tribological performance, lubrication, electrical conductivity, thermal resistance, and magnetic characteristics. Various materials, including metals, ceramics, polymers, cellulose, metal oxides, and nitrides, have been utilised in the electro-deposition process (Anyanwu *et al*., 2022; Odetola *et al*., 2016).

This process can be executed using two types of current: direct current (DC) and pulse current (PC). The key distinction between these methods lies in their current application; in direct current, a constant current is applied, whereas in pulse current, the electrical current alternates between two different values (Popoola and Fayomi, 2012; Odetola *et al*., 2016). While the properties of deposited coatings can be negatively impacted by the pulsating parameters in the electro-deposition process, better element dispersion and more uniform coatings, particularly in terms of throw power and edge coverage, have been reported with the direct current electro-deposition method (Odetola *et al*., 2016; Fayomi and Popoola, 2015).

Recent times have seen the successful application of metal oxide–biopolymer composite coatings to enhance the surface and structural integrity of low-carbon steel (Fayomi and Popoola, 2015) (Anyanwu *et al*., 2021a; Anyanwu *et al*., 2021b; Anyanwu *et al*., 2023b; Anyanwu *et al*. 2022). The co-deposition of nanoparticles, derived from metal oxides, cellulose, ceramics, nitrides, etc., on metallic substrates is becoming more and more popular as a way to improve the mechanical, corrosion, and thermal properties (Meulendijks *et al*., 2017; Anyanwu *et al*., 2021). Their incorporation provides enhanced corrosion resistance and self-lubricating qualities on the substrate (low-carbon steel). There are a lot of their nanoparticulates in the market that are used to create composite coatings for steel and other metals. Cellulose is the most widely used biopolymer at the moment, and it's also cheap (Chakraborty *et al*., 2005; Shi *et al*., 2011). Despite having significant potential, they are also environmentally friendly, and there are currently few studies on their electro-deposition. Because of their renewable, mechanical, corrosion-resistant, biocompatible, and biodegradable qualities, they have found widespread application in a variety of fields, including medication delivery, electrically conductive coatings, heavy metal removal, and adsorbent materials (Meulendijks *et al*., 2017).

According to Anyanwu *et al*., 2021; Anyanwu *et al*., 2021b; Meulendijks *et al*., 2017, their nanoparticles have been effectively co-deposited separately on low-carbon steel, silver, Ag, and copper, Cu metals. They can also be used in a wide range of home and industrial applications, such as wastewater treatment, organic and metallic coatings, and solar cells. Research by Mohanty *et al*. (2001), Anyanwu *et al*. (2021a), and Meulendijks *et al*. (2017) has reported that they have also been used to reinforce metallic coatings, with improved wear resistance, hardness, and other qualities like corrosion resistance.

The biopolymer (nano-cellulose) plant known as kenaf (Hibiscus cannabinus L.) grows effectively in a variety of soil conditions and needs little pesticide application. It is widely grown around the world, including Nigeria. 90% cellulose means that kenaf has good mechanical qualities and is rich in natural fibres (Jeyanthi *et al*., 2012; Anyanwu *et al*., 2019a, 2019b; Jonoobi *et al*., 2009). The technique has shown to be effective in the creation of

metal matrix composites, yielding exceptional outcomes (Anyanwu *et al*., 2021a; Shi *et al*., 2011).

This study was therefore aimed at depositing zinc-magnesium oxide-cellulose nano-particle coatings (Zn-xMgO-xC_n), on low-carbon steel (substrates), for improved corrosion resistance properties in sodium chloride media through a direct current (DC) electro-deposition route. The gravimetric technique was used to determine the corrosion rates of the deposited coatings. The surface morphologies of the composite coatings were determined by optical microscopy and a Tescan scanning electron microscopy enhanced with energy dispersive spectroscopy.

2. MATERIALS AND METHODS

2.1 Materials Preparation and Procedures

The primary materials and chemicals used in this study include a zinc bar measuring 30 mm x 20 mm x 4 mm (molecular weight: 65.38, purity: 99.9%, melting point: 420°C, boiling point: 907°C); 200g of magnesium oxide nanoparticles (MgO = 99.5%, CaO = 0.3%, Cl = 0.02%, Na = 0.02% and SO_4 = 0.16%; particle size = 20 - 80 nm; melting point = 2800 ºC; boiling point = 3600 ºC); analytical grade zinc chloride (purity: 98%, molecular weight: 136.29); glycine and thiourea.

The chemicals were all provided by a reliable chemical vendor in Ibadan, Nigeria. Additionally, about 150g of nano-cellulose fibres with a cellulose content of 95%, a particle size range of 10nm to 50nm, crystallinity index of 74% were sourced from an Agricultural Research Institute in Southwestern Nigeria. The nanoparticle blend was formed by mixing 20g of MgO with varying amounts (5g – 20g) of nano-cellulose fibres and 10% acidic ionic liquid (Anyanwu *et al*., 2023a). A steel dealer in Agbara, Lagos State, South-Western Nigeria, provided the low-carbon steel substrate (0.24–0.30% C) used in the study.

2.2 Preparation of Substrate and Coating Deposition

The low-carbon steel substrate was polished using emery papers up to 600 grit to remove any pre-existing impurities and ensure a mirror-like finish free from scale defects. Subsequently, it was sectioned into pieces measuring 50 mm x 20 mm x 2 mm as recommended in (Anyanwu *et al*., 2021; Popoola *et al*., 2016). The samples were degreased in trichloroethylene, rinsed with water, and then activated by immersion in a 10% HCl solution for 10 seconds. The bath solution consisted of analytical grade reagents and distilled water, containing zinc chloride (100 g/L), glycine (10 g/L), thiourea (10 g/L), magnesium oxide nanoparticles (20 g/L), and nano-cellulose fibres (ranging from 5 g/L to 20 g/L).

Table 1 displays the composition of the nanoparticles and the applied voltage. The 99.9% zinc bar served as the anode and the pretreated substrate as the cathode. The anode and cathode distances and immersion depth were maintained constant. To facilitate the admixture and complete dissolving of all particles, the bath solution was heated to and kept at 40 degrees Celsius. After that, it was constantly agitated at a speed of up to 1000 rpm using a mechanical stirrer to ensure the electrolytes were consistent.

For 20 minutes, the deposition was done with a fixed current density of 2.0 A/cm2, 5.5 pH, 0.3 and 0.5V set potentials, and changing nanoparticle concentrations. The samples were dried in the air after being rinsed in distilled water for five seconds following the deposition.

2.3 Corrosion behaviour of the coatings and substrate

The gravimetric approach was used to examine the corrosion behaviour of the substrate and the generated composite coatings. This was carried out in 3.5 wt% NaCl medium at ambient temperature. The methods used comply with ASTM G31-72, 2004 (Standard Practice for Laboratory Immersion Corrosion Testing of Metals) and ASTM 2003d (Standard Practice for Preparing, Cleaning, and Assessing Corrosion Test Specimens). A high precision Mettler Toledo analytical balance was used to weigh coupons that measured 1 centimetre by 1 centimetre before and after they were submerged in the corrosion media for 720, 1440, 2160, and 2880 hours, respectively. After that, the coupons were taken out, cleaned with acetone and water, and dried. The weight differential was measured and documented. Equations 1, 2 and 3 as recommended by (Anyanwu *et al*., 2021) were then used to calculate the corrosion rates, protection efficiencies, $E(\%)$ and degree of surface coverage (θ) of the samples.

$$CR = \frac{8.76 \times 10^4 \Delta W}{\rho A T} \quad \ldots\ldots(1)$$

$$E\,(\%) = (1 - \frac{CR_C}{CR}) \times 100 \quad \ldots.(2)$$

$$\theta = (1 - \frac{CR_C}{CR}) \quad \ldots\ldots\ldots(3)$$

Where W= Weight loss (g), ρ = Density of the sample (g/mm^3), A = Exposed area (cm^2), T = Exposure time (hours), CR_C = corrosion rate when coating was employed (mm/year) and CR = corrosion rate without the coatings in mm/year (i.e. the corrosion rate of the substrate).

24 Morphology of the coatings and substrate

The samples' surface morphologies were determined via a 400X magnification optical microscope after corrosion analysis. Additionally, a 1000X magnification TESCAN scanning electron microscope, equipped with energy dispersive spectroscopy (SEM/EDS), was used to analyse the microstructures of the produced coatings and substrate. The EDS was used to verify the composition of the as-received substrate.

3. RESULTS AND DISCUSSION

3.1 Corrosion behaviour of the samples

The result of the corrosion behaviour of the samples is presented in Tables 2-3 and Figures 1-2. From the table, it is evident that as the coupons' exposure time in the corrosive media increases, the corrosion rate values for all samples decrease. Also, an increase in the deposition voltage and concentration of the nanoparticle blends reduces the corrosion rate values. This might be attributed to the effectiveness of the nanoparticle layer coating on the mild steel surface.

At higher voltage, there is an increase in the electron transfer in the bath, thereby improving coating uniformity. These layers likely inhibit direct contact between chloride ions and the substrate surface, thereby reducing the formation of corrosion products (Anyanwu *et al*., 2023; Anyanwu *et al*., 2022; Fayomi *et al*., 2021a). The layers often work to keep the chloride ions from

coming into direct contact with the substrate's surface, which lessens the likelihood that corrosion products would occur, as evident in (Anyanwu *et al*., 2023b; Anyanwu *et al*., 2022; Fayomi *et al*., 2021). According to Tables 2 and 3, the corrosion rate values are functions of the samples' corresponding mass loss, which increases for every sample as the exposure time increases. Also, as seen from the table, all the samples provided values for corrosion rates lower than those of the "as-received" sample, "A." The findings further revealed that sample M10 (Zn-20gMgO-20gC_n) had the lowest average corrosion rate value (0.2582 mm/y). In contrast to the 'as-received' sample, which had an average corrosion rate value of 5.0025 mm/y, the sample provided 95% protection efficiency and 0.95 degree of surface coverage on the substrate (Figure 1-2). Sample M7 (Zn-20gMgO-5gCn) had the greatest corrosion rate value of 2.2236 mm/y, the maximum protection efficacy of 56%, and the degree of surface coverage of 0.56 among the coating samples (Figure 1-2).

It can thus be concluded that the corrosion rate decreases with an increase in the concentration or combination of nanoparticles, a trend that is consistent with findings reported in similar literature (Zhang *et al*., 2013; Anyanwu *et al*., 2023b; Anyanwu *et al*., 2022; Ahmad and Salam, 2019).

Table 1: Composition of the nanoparticle blends

Experiment no.	Nanoparticles blend	Voltage (V)	Sample ID
1	Zn-20gMgO-5gC_n	0.3	M2
2	Zn-20gMgO-10gC_n	0.3	M3
3	Zn-20gMgO-15gC_n	0.3	M4
4	Zn-20gMgO-20gC_n	0.3	M5
5	Zn-20gMgO-5gC_n	0.5	M7
6	Zn-20gMgO-10gC_n	0.5	M8
7	Zn-20gMgO-15gC_n	0.5	M9
8	Zn-20gMgO-20gC_n	0.5	M10
9	As received low carbon steel substrate (Control)	-	A

Table 2. Corrosion data of the substrate and deposited coatings at 0.3V

Time	720 Hours		1440 Hours		2160 Hours		2880 Hours		Ave. C.R
Sample	ΔW	C.R	ΔW	C.R	ΔW	C.R	ΔW	C.R	**(mm/y)**
ID	(g)	(mm/y)	(g)	(mm/y)	(g)	(mm/y)	(g)	(mm/y)	
M2	0.1260	1.9574	0.2450	1.9040	0.3611	1.8673	0.4801	1.8594	1.8971
M3	0.1080	1.6712	0.2091	1.6212	0.3090	1.5981	0.4021	1.5562	1.6117
M4	0.0390	0.6001	0.0721	0.5612	0.1010	0.5222	0.1250	0.4842	0.5419
M5	0.0130	0.1993	0.0210	0.1604	0.0251	0.1304	0.0291	0.1103	0.6004
A	0.3950	6.1215	0.7731	5.9931	0.7891	4.0767	0.9855	3.8185	5.0025

Table 3. Corrosion data of the substrate and deposited coatings at 0.5V

Time	**720 Hours**		**1440 Hours**		**2160 Hours**		**2880 Hours**		**Ave. C.R**
Sample	ΔW	C.R	ΔW	C.R	ΔW	C.R	ΔW	C.R	**(mm/y)**
ID	(g)	(mm/y)	(g)	(mm/y)	(g)	(mm/y)	(g)	(mm/y)	
M7	0.1471	2.2851	0.2911	2.2548	0.4290	2.2164	0.5511	2.1379	2.2236
M8	0.0841	1.3012	0.1661	1.2867	0.2390	1.2342	0.2550	0.9864	1.2021
M9	0.0230	0.3565	0.0400	0.3102	0.0570	0.2945	0.0740	0.2886	0.3125
M10	0.0200	0.3024	0.0390	0.2994	0.0451	0.2298	0.0521	0.2010	0.2582
A	0.3950	6.1215	0.7731	5.9931	0.7891	4.0767	0.9855	3.8185	5.0025

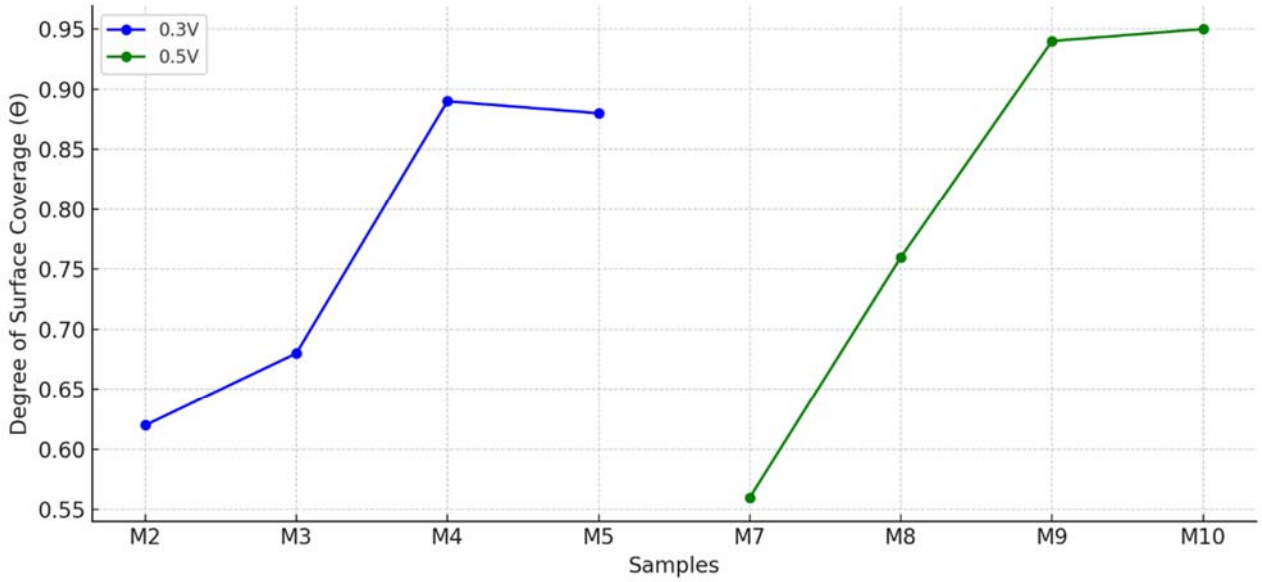

Figure 1. Degree of surface coverage for the coatings deposited at 0.3V and 0.5V.

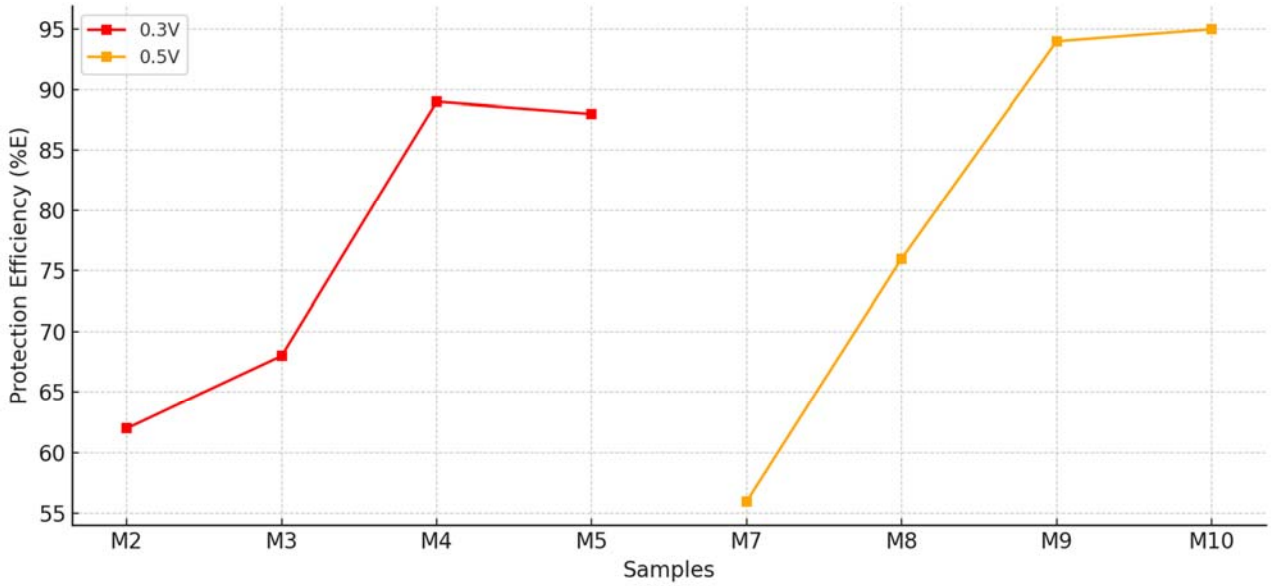

Figure 2: Protection efficiency for the coatings deposited at 0.3V and 0.5V.

The corrosion mechanism here includes the formation of corrosion products (iron hydroxide), dissolution of iron ions, creation of ferrous chloride, acidification of the solution, and the generation of hydrogen gas (Fontana, 1986; Patra, 2019). They are summarized on equations 4 – 9. Formation of iron oxide

$$Fe + 2H_2O + O_{2(g)} \rightarrow Fe(OH)_3 \ldots\ldots (4)$$

In the presence of oxygen (O_2) and water (H_2O), iron (Fe) reacts to form iron hydroxide $Fe(OH)_3$, which is commonly known as corrosion products /rust. This is then followed by the dissolution of iron ions:

$$Fe(OH)_3 + 3H^+ \rightarrow Fe^{3+} + 3H_2O \ldots\ldots (5)$$

The iron hydroxide ($Fe(OH)_3$) formed in the previous step reacts with hydrogen ions (H^+) to form iron ions (Fe^{3+}) and water (H_2O). This is followed by the formation of ferrous chloride:

$$Fe + 2Cl^- \rightarrow FeCl_2 \ldots\ldots\ldots\ldots (6)$$

Iron (Fe) reacts with chloride ions (Cl-) to form ferrous chloride (FeCl2), followed by the acidification of the solution:

$$H_2O \rightarrow H^+ + OH^- \ldots\ldots\ldots\ldots\ldots (7)$$

Water (H_2O) dissociates into hydrogen ions (H+) and hydroxide ions (OH-), followed by the formation of hydrogen gas:

$$2H^+ + 2e^- \rightarrow H_2 \ldots\ldots\ldots\ldots (8)$$

Hydrogen ions (H^+) gain electrons (e^-) to form hydrogen gas (H_2). Overall reaction:

$$Fe + 2H_2O + 2Cl^- + O_2 \rightarrow FeCl_2 + 3H_2O + H_2 . (9)$$

Corrosion results from ion migration from the substrate's surface to the bulk of the solution when the samples come into contact with the corrosive media. The protective nanoparticle coatings on the substrate, however, obstruct this migration and prevent the samples and corrosive media from reacting further. The substrate sample's corrosion rates are greatly reduced by this action.

3.1 Morphology of the samples

The SEM/EDS spectrum of the low-carbon steel sample (substrate) as received is displayed in Figure 3. As can be seen, the carbon level (0.26%) of the steel is within allowable limits as recommended by the ASTM standard code (Anyanwu *et al*., 2023a; Mahto *et al*., 2023). The SEM and EDS spectra of the sample coatings made from the nano-cellulose particles (xMgO-xCn) are displayed in Figure 4, which is a representative figure.

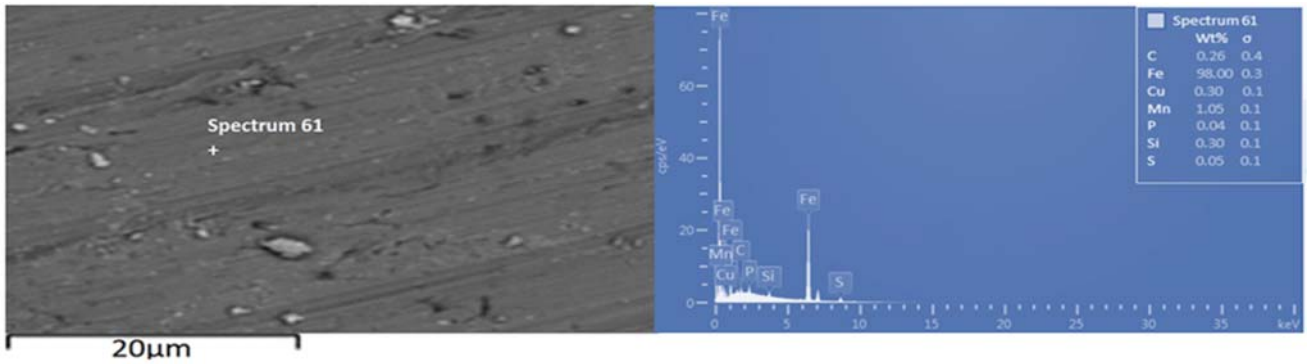

Figure 3: SEM / EDS Spectra of the as received low carbon steel

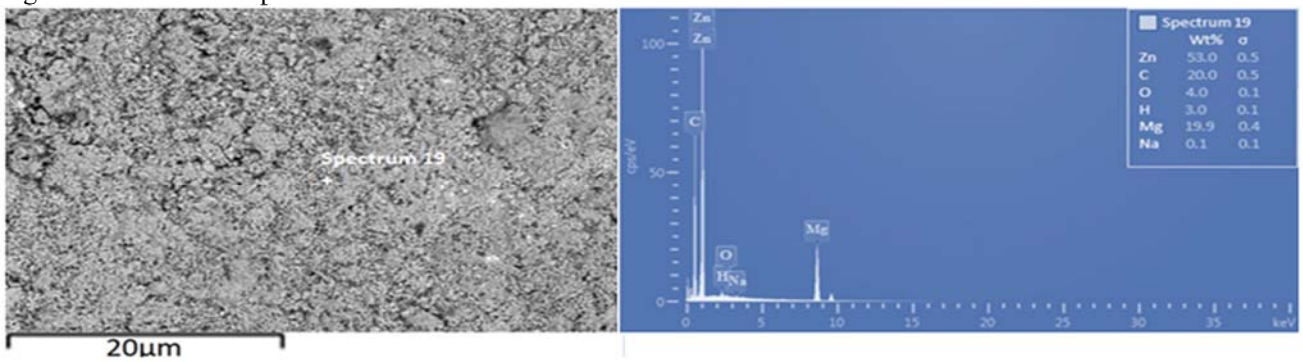

Figure 4: SEM/EDS imaging of the deposited 20gMgO-20gC_n composite Coatings.

Before the corrosion investigation, the picture and spectrum were captured. Each coating exhibited good adhesion to the substrate, well-spaced grains, and no porosity (see representation on Figure 4). Sample M10 had superior coatings properties, though. Given that the nano-particles mixes were more evenly distributed and deposited on the substrate, this may be explained by their higher concentration in the bath (Popoola *et al*., 2016; Sajjadnejad *et al*., 2021).

Additionally, they demonstrated strong throw power and edge protection, both of which support and improve the coating's structural integrity and performance. Zinc, Zn, magnesium, Mg, carbon, C, and trace amounts of oxygen, O, and hydrogen, H were present in the compositions of all the coating samples (Figure 4). The nano-cellulose particles that were utilised may have contributed to the carbon, oxygen, and hydrogen levels (Anyanwu *et al*., 2022; Cherian *et al*., 2022).

The optical microscopic (OPM) images of the generated sample coatings and substrate (C) are displayed in Figure 5. The images were taken after the samples were exposed to the corrosive media. It clear from the images that the "as received sample" had a significant corrosive effect due to the corrosive media's attack.

There are more corrosive compounds produced on its surface than on the developed coatings' surfaces. On the surfaces of the produced coatings, a small number of pitting corrosion spots were observed, particularly on sample M10 (20gMgO-20gCn). This might have something to do with the sample's improved coating adherence, edge coverage, and coating throw power, as seen by the SEM spectra. Research has demonstrated that coatings with sufficient throw power, strong adhesion, and effective edge coverage provide excellent performance in service (Anyanwu *et al*., 2023a; Popoola *et al*., 2016; Fayomi *et al*., 2017).

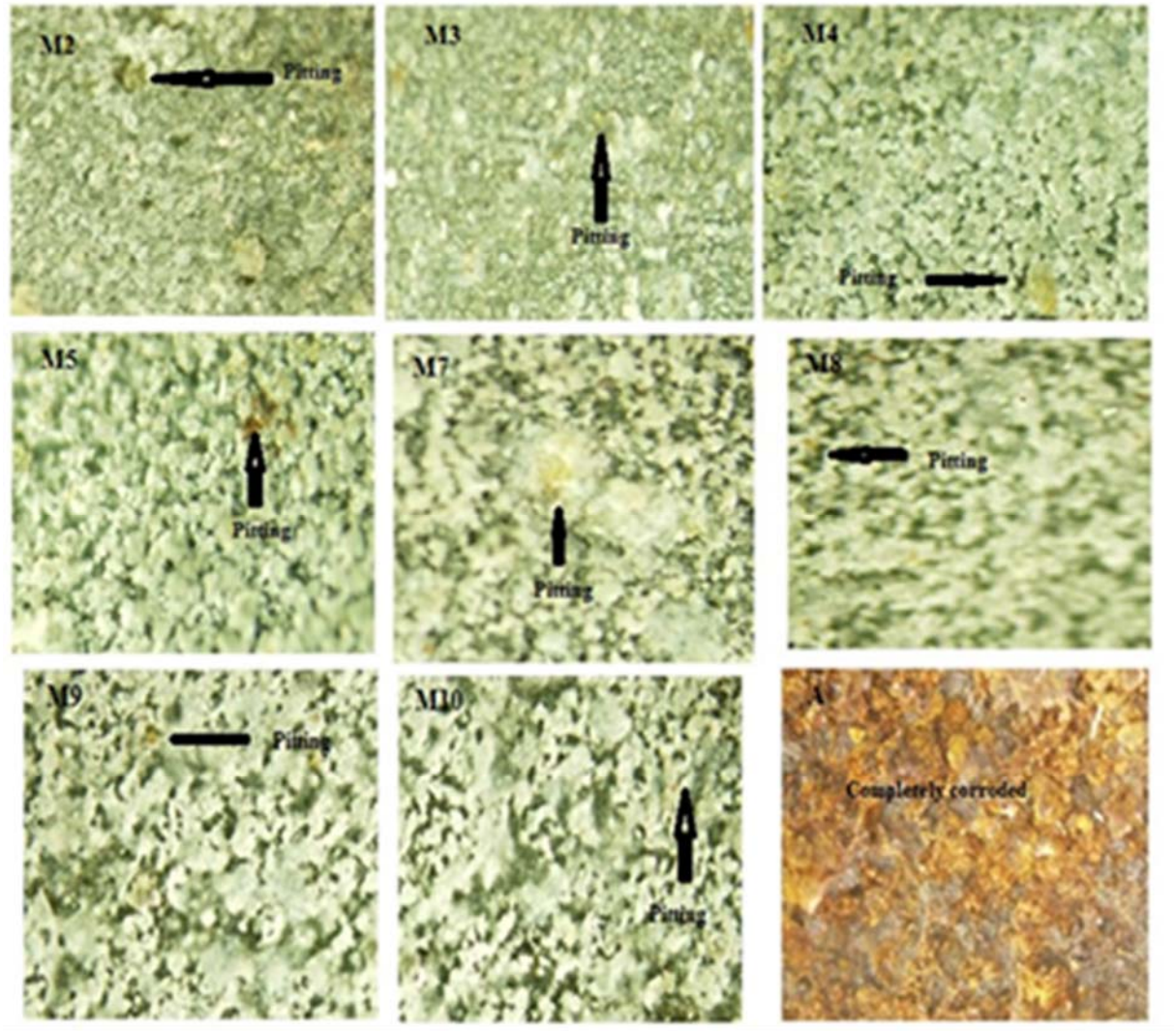

Figure 5: OPM images of all samples after exposure in the corrosive media

4.0 CONCLUSION

The zinc-magnesium oxide-cellulose nanoparticles (Zn-xMgO-xCn) were successfully deposited onto low carbon steel substrates using the electrodeposition process. The coatings exhibited good throw power, edge coverage, homogeneity, and coating adhesion in the sample. This explained why their corrosion rate values were lower than those of the low carbon steel sample used in the investigation. The sample with the lowest corrosion rate value 0.2582 mm/y, M10 (20gMgO-20gCn), had a protection efficacy of 95% on the low carbon steel. According to the study, the zinc-magnesium oxide-cellulose nanoparticle coatings prevented a subsequent reaction that would have intensified the low carbon steel sample's corrosion by preventing the migration of chloride ions to the substrate. This resulted in a considerable decrease in corrosion rates and an improvement in the sample's corrosion resistance.

Acknowledgement

The researchers acknowledged the support of the following bodies in starting and executing the study: Management of Federal University of Agriculture, Abeokuta, Ogun State, Nigeria. Tertiary Education Trust Fund (TetFund), Nigeria, Management of Tshwane University of Technology, Pretoria, South Africa

REFERENCES

Abbas, M., and Shafiee, M. (2020). An overview of maintenance management strategies for corroded steel structures in extreme marine environments. *Marine Structures*, *71*, 102718. https://doi.org/10.1016/j.marstruc.2020.102718

Anyanwu, B. U., Oluwole, O. O., Fayomi, O. S., and et, al. (2023a). Assessing the impact of Zn-MgO-xCn Ternary Coatings on A36 Low Carbon Steels for Oil and Gas Pipeline Applications. *Portugaliae Electrochimica Acta*, *41*(4), 301–313. https://doi.org/10.4152/pea.2023410404

Anyanwu, B. U., Oluwole, O. O., Fayomi, O. S., and et, al. (2023b). Assessing the impact of Zn-MgO-xCn Ternary Coatings on A36 Low Carbon Steels for Oil and Gas Pipeline Applications. *Portugaliae Electrochimica Acta*, *41*(4), 301–313. https://doi.org/10.4152/pea.2023410404

Anyanwu B.U; Oluwole O.O; Fayomi O.S.I; Olorunnisola A.O; Kuye S.I; Owoeye S.O and Olamide O.O. (2022). *Polarization Corrosion Effects of Nanocellulose Reinforced Zinc-Magnesium Oxide Coatings on A36 Steel in Acidic Media. International Journal of Basic Science and Technology 8(3): 168-177.*

Anyanwu, B. U., Oluwole, O. O., Fayomi, O. S. I., Olorunnisola, A. O., Popoola, A. P. I., and Kuye, S. I. (2021a). Processing and Development of Corrosion Resistance Surface-Active Thin Film Nanocellulose Composite Coatings for Mild Steel Protection. *Protection of Metals and Physical Chemistry of Surfaces*, *57*(6), 1206–1213. https://doi.org/10.1134/S2070205121060034

Anyanwu, B. U., Oluwole, O. O., Fayomi, O. S. I., Olorunnisola, A. O., Popoola, A. P. I., and Kuye, S. I. (2021b). Synthesis, corrosion and structural characterization of kenaf nanocellulose on Zn–ZnO-Cn electrolytic coatings of mild steel for advanced applications. *Case Studies in Chemical and Environmental Engineering*, *3*, 100017. https://doi.org/10.1016/j.cscee.2020.100017

Anyanwu B.U, O.O. Oluwole, O.S.I. Fayomi, A.O. Olorunnisola, A.P.I. Popoola, and S.I. Kuye. (2021). *Synthesis, corrosion and structural characterization of kenaf nanocellulose on Zn-ZnO-xCn electrolytic coatings of mild steel for advanced applications. Case Studies in Chemical and Environmental Engineering. 3:1-5. doi.org/10.1016/j.cscee.2020.100017.*

A.P.I. Popoola, and O.S.I. Fayomi. (2012). *Performance evaluation of zinc deposited mild steel in chloride medium, Int. J. Electrochem. Sci., 6 : 3254-3326.*

A.P.I. Popoola, V.S. Aigbodion, and O.S.I. Fayomi. (2016). *Surface characterization, mechanical properties and corrosion behaviour of ternary based Zn-ZnO-SiO2 composite coating of mild steel, Journal of Alloys and Compounds, 654 : 561-566.*

B.M. Praveeen., and T.V. Venkatesh. (2011). *Electro-deposition and corrosion resistance properties of Zn-Ni/Tio2 nano composite coating, Int. J. Electrochem, 261 : 407-792.*

Cai, Y., Xu, Y., Zhao, Y., and Ma, X. (2020). Atmospheric corrosion prediction: a review. *Corrosion Reviews*, *38*(4), 299–321. https://doi.org/10.1515/corrrev-2019-0100

Chakraborty, A., Sain, M., and Kortschot, M. (2005). Cellulose microfibrils: A novel method of preparation using high shear refining and cryocrushing. *Holzforschung*, *59*(1), 102–107. https://doi.org/10.1515/HF.2005.016

Cherian, R. M., Tharayil, A., Varghese, R. T., Antony, T., Kargarzadeh, H., Chirayil, C. J., and Thomas, S. (2022). A review on the emerging applications of nano-cellulose as advanced coatings. *Carbohydrate Polymers*, *282*, 119123. https://doi.org/10.1016/j.carbpol.2022.119123

El-Sherik. (2016). *The effect of chloride ion concentration on the corrosion behavior of mild steel in alkaline medium. Journal of Materials Science and Chemical Engineering, 4(5), 1-9.*

Fan, X., Wang, X., Ji, Z., Li, X., Gan, M., Wang, Y., Zheng, H., Chen, X., Sun, Z., and Huang, X. (2022). Physico-chemical profile and corrosion mechanism of the failure grate bar from iron ore sintering process. *Journal of Materials Research*

and Technology, *20*, 428–439. https://doi.org/10.1016/j.jmrt.2022.07.130

Fayomi, O. S. I., Ayodeji, S. A., Anyanwu, B. U., Nkiko, M. O., and Dauda, K. T. (2021). Effect of Electrodeposition Mechanism and α-Siandlt;subandgt;3andlt;/subandgt;Nandlt;subandgt;4andlt;/subandgt;/ZrBrandlt;subandgt;2andlt;/subandgt; Doped Composite Particle on the Physicochemical and Structural Properties of Processed NiPZn Coatings on Mild Steel for Advance Application. *Key Engineering Materials*, *900*, 61–73. https://doi.org/10.4028/www.scientific.net/KEM.900.61

Feng, W., Tarakbay, A., Ali Memon, S., Tang, W., and Cui, H. (2021). Methods of accelerating chloride-induced corrosion in steel-reinforced concrete: A comparative review. *Construction and Building Materials*, *289*, 123165. https://doi.org/10.1016/j.conbuildmat.2021.123165

F. Zhang. (2015). *Effect of chloride ion concentration on the corrosion behavior of mild steel in simulated concrete pore solutions. Construction and Building Materials, 93, 114-121.*

Ibrahimi, B. El, Nardeli, J. V., and Guo, L. (2021). *An Overview of Corrosion* (pp. 1–19). https://doi.org/10.1021/bk-2021-1403.ch001

Mahto, M. K., Kumar, A., Vashista, M., and Khan Yusufzai, M. Z. (2023). Corrosion behaviour of copper cladded steel produced using multi pass friction stir welding process. *CIRP Journal of Manufacturing Science and Technology*, *47*, 244–259. https://doi.org/10.1016/j.cirpj.2023.10.006

Meulendijks, N., Burghoorn, M., van Ee, R., Mourad, M., Mann, D., Keul, H., Bex, G., van Veldhoven, E., Verheijen, M., and Buskens, P. (2017). Electrically conductive coatings consisting of Ag-decorated cellulose nanocrystals. *Cellulose*, *24*(5), 2191–2204. https://doi.org/10.1007/s10570-017-1240-y

Mi, T., Li, Y., Liu, W., Dong, Z., Gong, Q., Min, C., Xing, F., Wang, Y., and Chu, S. H. (2023). The effect of carbonation on chloride redistribution and corrosion of steel reinforcement. *Construction and Building Materials*, *363*, 129641. https://doi.org/10.1016/j.conbuildmat.2022.129641

Obot, I. B., Sorour, A. A., Verma, C., Al-Khaldi, T. A., and Rushaid, A. S. (2023). Key parameters affecting sweet and sour corrosion: Impact on corrosion risk assessment and inhibition. *Engineering Failure Analysis*, *145*, 107008. https://doi.org/10.1016/j.engfailanal.2022.107008

Odetola, P., Popoola, P., Popoola, O., and Delport, D. (2016). Parametric Variables in Electro-deposition of Composite Coatings. In *Electrodeposition of Composite Materials*. InTech. https://doi.org/10.5772/62010

O.S.I. Fayomi, and A.P.I. Popoola. (2015). *Development of smart oxidation and corrosion resistance of multi-doped complex hybrid coatings on mild steel, J. Alloys Compd. 637 : 382–392.*

O.S.I. Fayomi, O.O. Joseph, and A.P.I. Popoola. (2017). *Structural properties and micro-hardness performance of induced composite coatings filled with cocosnucifera-tin functionalized oxide, Energy Proceedia, 119 : 910-915.*

P. Patra. (2019). *Influence of pH on the corrosion behavior of mild steel in NaCl solution. Materials Today: Proceedings, 15, 225-231.*

Sajjadnejad, M., Haghshenas, S. M. S., Badr, P., Setoudeh, N., and Hosseinpour, S. (2021). Wear and tribological characterization of nickel matrix electrodeposited composites: A review. *Wear*, *486–487*, 204098. https://doi.org/10.1016/j.wear.2021.204098

Sanders, D. M., and Anders, A. (2000). Review of cathodic arc deposition technology at the start of the new millennium. *Surface and Coatings Technology*, *133–134*, 78–90. https://doi.org/10.1016/S0257-8972(00)00879-3

Shi, J., Shi, S. Q. , Barnes, H. M., and Pittman, C. U. ,. (2011). *A chemical process for preparing cellulosic fibers hierarchically from kenaf bast fibers. BioResources, 6(1), pp.879-890.*

Smith, L., and Craig, B. (2020). *Corrosion mechanisms and material performance in environments containing hydrogen sulfide and elemental sulfur. In Sulphur-Assisted Corrosion in Nuclear Disposal Systems (pp. 46-65). CRC Press.*

Song, Y., Jiang, G., Chen, Y., Zhao, P., and Tian, Y. (2017). Effects of chloride ions on corrosion of ductile iron and carbon steel in soil environments. *Scientific Reports*, *7*(1), 6865. https://doi.org/10.1038/s41598-017-07245-1

Tay, B. K., Zhao, Z. W., and Chua, D. H. C. (2006). Review of metal oxide films deposited by filtered cathodic vacuum arc technique. *Materials Science and Engineering: R: Reports*, *52*(1–3), 1–48. https://doi.org/10.1016/j.mser.2006.04.003

Wasim, M., Shoaib, S., Mubarak, N. M., Inamuddin, and Asiri, A. M. (2018). Factors influencing corrosion of metal pipes in soils. *Environmental Chemistry Letters*, *16*(3), 861–879. https://doi.org/10.1007/s10311-018-0731-x

Zehra, S., Mobin, M., and Aslam, J. (2022). An overview of the corrosion chemistry. In *Environmentally Sustainable Corrosion Inhibitors* (pp. 3–23). Elsevier. https://doi.org/10.1016/B978-0-323-85405-4.00012-4